BPS Dendroscopy on Local del Pezzo surfaces

Boris Pioline

Workshop on Enumerative Invariants, Quantum Fields and String Theory Correspondences

Mittag-Leffler Institute, 25/7/2024

Thanks to my wonderful co-authors

  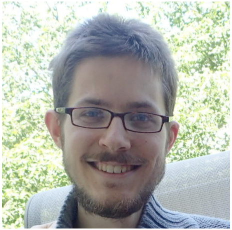 

Based on 'BPS Dendroscopy on Local $\mathbb{P}^2$' [2210.10712]
with Pierrick Bousseau, Pierre Descombes and Bruno Le Floch

and 'BPS Dendroscopy on Local $\mathbb{F}_0$' with Bruno Le Floch and Rishi Raj, to appear

δενδρον= tree

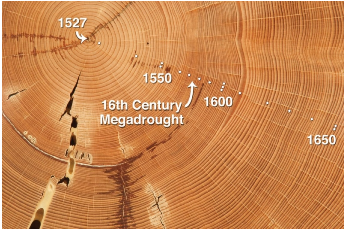

Dendrochronology

Dentrology

Dentrobate

δενδρο- scopy

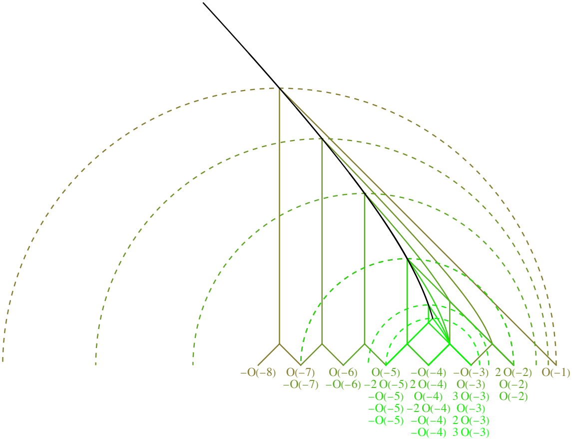

$$\Omega(\text{Hilbert scheme of 7 points on } \mathbb{P}^2) = \sum_{7 \text{ trees}} = 429$$

Introduction

- In type IIA string theory compactified on a Calabi-Yau threefold X, the BPS spectrum consists of bound states of D6-D4-D2-D0 branes, with charge $\gamma \in H_{\rm even}(X,\mathbb{Q})$.
- BPS states saturate the bound $M(\gamma) \geq |Z(\gamma)|$, where the central charge $Z \in \mathrm{Hom}(\Gamma,\mathbb{C})$ depends on the complexified Kähler moduli.
- The index $\Omega_z(\gamma)$ counting BPS states is robust under complex structure deformations, but in general depends on $z \in \mathcal{M}_K$.
- Mathematically, the Donaldson-Thomas invariant $\Omega_z(\gamma)$ counts stable objects with $\mathrm{ch}\, E = \gamma$ in the derived category of coherent sheaves $\mathcal{C} = D^b\mathrm{Coh}(X)$, and depend on a choice of Bridgeland stability condition $z \in \mathrm{Stab}\,\mathcal{C} \supset \mathcal{M}_K$.
- Physics/Mirror symmetry selects a particular slice $\Pi \subset \mathrm{Stab}\,\mathcal{C}$ isomorphic to $\widetilde{\mathcal{M}_K}$. It is sometimes advantageous to consider other slices, e.g. tilt-stability or large volume slice.

Introduction

- $\Omega_z(\gamma)$ is locally constant on $\mathrm{Stab}\,\mathcal{C}$, but can jump across real codimension one walls of marginal stability $\mathcal{W}(\gamma_L, \gamma_R)$, where the phases of the central charges $Z(\gamma_L)$ and $Z(\gamma_R)$ become aligned *[Kontsevich Soibelman'08, Joyce Song'08]*
- Physically, multi-centered black hole solutions with charges $\gamma = m_L\gamma_L + m_R\gamma_R$ (dis)appear across the wall

$$r = \frac{\langle\gamma_L, \gamma_R\rangle\, |Z(\gamma_L + \gamma_R)|}{\mathrm{Im}[\bar{Z}(\gamma_L)\, Z(\gamma_R)]}$$

$$\Delta\Omega(\gamma_L + \gamma_R) = \pm\, |\langle\gamma_L, \gamma_R\rangle|\, \Omega(\gamma_L)\Omega(\gamma_R)$$

Denef'02, Denef Moore '07, ...

Introduction

- The spectrum is expected to simplify along the gradient flow for the mass $|Z(\gamma)|$, aka attractor flow *[Ferrara Kallosh Strominger'95]*

$$\mathrm{AF}_\gamma : \quad r^2 \frac{\mathrm{d}z^a}{\mathrm{d}r} = -g^{a\bar{b}} \partial_{\bar{b}} |Z_z(\gamma)|^2$$

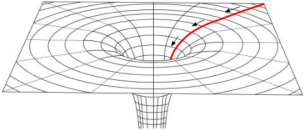

- Since $|Z_z(\gamma)|$ decreases along the flow, $z(r \to \infty)$ can either reach a regular local minimum of $|Z_z(\gamma)| > 0$ inside $\mathrm{Stab}\,\mathcal{C}$, or a point on the boundary where $Z_z(\gamma) = 0$.
- We define the attractor point $z_\star(\gamma)$ as the endpoint of the flow, and the attractor invariant as $\Omega_\star(\gamma) = \Omega_{z_\star(\gamma)}(\gamma)$. An additional label might be necessary in case of multiple basins of attraction.

The Split Attractor Flow Conjecture

- Starting from $z \in \widetilde{\mathcal{M}_K}$, following AF_γ and recursively applying the WCF formula whenever the flow crosses a wall of marginal stability, one can *in principle* express $\Omega_z(\gamma)$ in terms of attractor invariants $\Omega_\star(\gamma_i)$.

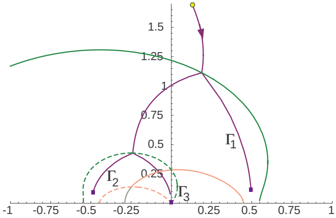

Denef Moore'07

The Split Attractor Flow Conjecture (SFAC)

- In terms of the rational DT invariants *[Joyce Song 08, Manschot BP Sen 11]*

$$\bar{\Omega}_z(\gamma) := \sum_{k|\gamma} \frac{y-1/y}{k(y^k-y^{-k})} \Omega_z(\gamma/k)_{y\to y^k} \overset{y\to 1}{\to} \sum_{k|\gamma} \frac{1}{k^2} \Omega_z(\gamma/k)$$

  the result takes the form

$$\bar{\Omega}_z(\gamma) = \sum_{\gamma=\sum\gamma_i} \frac{g_z(\{\gamma_i\},y)}{\mathrm{Aut}(\{\gamma_i\})} \prod_i \bar{\Omega}_\star(\gamma_i)$$

  where $g_z(\{\gamma_i\},y)$ is a sum over attractor flow trees.
- The Split Attractor Flow Conjecture is the statement that for any $z \in \mathcal{M}_K$, only a finite number of decompositions $\gamma = \sum \gamma_i$ contribute to the index $\bar{\Omega}_z(\gamma)$.

Denef'00, Denef Greene Raugas'01,Denef Moore'07

The Split Attractor Flow Conjecture

- Unfortunately it is not clear a priori which constituents γ_i can contribute, except for the obvious constraints

$$\sum_i \gamma_i = \gamma \ , \quad \sum_i |Z_{z_\star(\gamma_i)}(\gamma_i)| < |Z_z(\gamma)|$$

- In particular, there can be cancellations between D-branes and anti-D-branes, and contributions from conifold states which are massless at their attractor point are difficult to bound.
- Even if SAFC holds, one still has to compute the attractor indices $\Omega_\star(\gamma)$, a tall order for compact CY3, which generally admit regular attractor points.
- For non-compact CY3, several simplifications render the problem tractable.

Simplifications for local CY3

- First, because the central charge $Z_z(\gamma)$ is holomorphic, $|Z_z(\gamma)|^2$ has no local minima so the only attractor points are conifold points with $Z_z(\gamma_i) = 0$.
- Second, the phase of $Z(\gamma)$ is conserved along the attractor flow:

$$r^2 \frac{\mathrm{d}}{\mathrm{d}r} \log \frac{Z(\gamma)}{\bar{Z}(\gamma)} = -\partial_a Z(\gamma) g^{a\bar{b}} \partial_{\bar{b}} \bar{Z}(\gamma) + \partial_a Z(\gamma) g^{a\bar{b}} \partial_{\bar{b}} \bar{Z}(\gamma) = 0$$

The BPS spectrum for fixed phase is conveniently encoded in the scattering diagram $\mathcal{D}_\psi = \cup_\gamma \mathcal{R}_\psi(\gamma)$, i.e. the union of active rays

$$\mathcal{R}_\psi(\gamma) = \{z \in \mathrm{Stab}\,\mathcal{C}, \Omega_z(\gamma) \neq 0, \arg Z(\gamma) = \psi + \tfrac{\pi}{2}\}$$

The WCF gives strong consistency conditions when rays intersect.

Simplifications for local CY3

- Third, $\mathcal{C} = D^b \operatorname{Coh}(X)$ is isomorphic (in many ways) to the derived category of representations $D^b \operatorname{Rep}(Q, W)$ of certain quivers with potential, associated to exceptional collections on X. Physically, quiver nodes correspond to fractional branes with $\Omega_\star(\gamma_i) = 1$.
- In "quiver regions" where the objects of charge γ_i are stable and the central charges $Z(\gamma_i)$ lie in a common half-plane, the BPS spectrum reduces to the SUSY vacua of Quiver Quantum mechanics, or mathematically to harmonic forms on the moduli space of semi-stable representations of (Q, W).
- Finally, one can argue that the only attractor-stable BPS states are those associated to the nodes of the quiver, i.e. $\Omega_\star(\gamma) = 0$ unless $\gamma = \gamma_i$ *[Beaujard Manschot BP'20]*. This determines the scattering diagram in the quiver regions, and everywhere by consistency.

Outline

- In this talk, I will explain how to use these techniques to determine the BPS spectrum at any $z \in \mathtt{Stab}\, C$ for the simplest examples of CY threefolds, namely $X = K_S$ for $S = \mathbb{P}^2$ and $S = \mathbb{F}_0 = \mathbb{P}^1 \times \mathbb{P}^1$.
- We first construct the scattering diagram along the large volume slice, where the central charge is given by the classical expression $Z(\gamma) = -\int_S e^{-zH}\,\mathrm{ch}(E)$, quadratic in z.
- We then include corrections from worldsheet instantons and construct the scattering diagram on the physical slice Π.
- The resulting diagram interpolates between the quiver and large volume scattering diagrams, and is manifestly invariant under the action of the modular group $\Gamma_1(3)$ for $S = \mathbb{P}^2$, or $\Gamma_1(4)$ for $S = \mathbb{F}_0$.

Scattering diagram for quivers

- Let (Q, W) a quiver with potential, $\gamma = (N_1, \dots, N_K) \in \mathbb{N}^{Q_0}$ a dimension vector and $\theta = (\theta_1, \dots, \theta_K) \in \mathbb{R}^{Q_0}$ a (King) stability parameter such that $(\theta, \gamma) := \sum N_i \theta_i = 0$.
- This data defines a supersymmetric quantum mechanics with 4 supercharges, gauge group $G = \prod_i U(N_i)$, superpotential W, FI parameters θ_i. SUSY vacua are harmonic forms on

$$\mathcal{M}_\theta(\gamma) = \{ \sum_{a:i\to j} |\Phi_a|^2 - \sum_{a:j\to i} |\Phi_a|^2 = \theta_i, \quad \partial_{\Phi_a} W = 0\}/G$$

- Mathematically, $\mathcal{M}_\theta(\gamma)$ is the moduli space of θ-semi-stable representations of (Q, W) (i.e. $(\theta, \gamma') \leq (\theta, \gamma)$ for any subrep) and the refined BPS index $\Omega_\theta(\gamma, y)$ is (roughly) its Poincaré polynomial.
- $\Omega_\theta(\gamma, y)$ may jump on real codimension 1 walls when the inequality is saturated (and on complex codimension 1 loci when W is varied, but we keep W fixed) .

Scattering diagram for quivers

- The BPS indices are conveniently encoded in the stability scattering diagram $\mathcal{D}(Q, W)$,[Bridgeland'16], defined as the union of the real codimension-one rays $\{\mathcal{R}(\gamma), \gamma \in \mathbb{N}^{Q_0}\}$

$$\mathcal{R}(\gamma) = \{\theta \in \mathbb{R}^{Q_0} : (\theta, \gamma) = 0,\ \bar{\Omega}_\theta(\gamma) \neq 0\}$$

- Each point along $\mathcal{R}(\gamma)$ is equipped with an automorphism of the quantum torus algebra,

$$\mathcal{U}_\theta(\gamma) = \exp\left(\frac{\bar{\Omega}_\theta(\gamma)}{y^{-1}-y}\mathcal{X}_\gamma\right) \ , \quad \mathcal{X}_\gamma \mathcal{X}_{\gamma'} = (-y)^{\langle\gamma,\gamma'\rangle}\mathcal{X}_{\gamma+\gamma'}$$

  where $\langle\gamma,\gamma'\rangle := \sum_{a:i\to j}(N_i N'_j - N_j N'_i)$.

- The WCF ensures that the diagram is consistent: for any generic closed path $\mathcal{P} : t \in [0,1] \to \mathbb{R}^{Q_0}$, $\prod_i \mathcal{U}_{\theta(t_i)}(\gamma_i)^{\epsilon_i} = 1$

Scattering diagram for Kronecker quiver

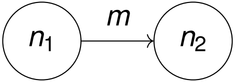

$$\theta_1 > 0, \theta_2 < 0 : \quad \dim \mathcal{M}_\theta(\gamma) = m n_1 n_2 - n_1^2 - n_2^2 + 1$$

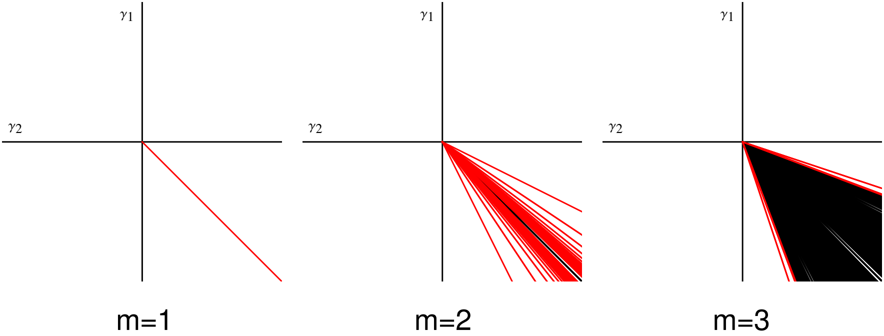

Attractor invariants for quivers

- The analogue of the attractor point for quivers is the self-stability condition *[Manschot BP Sen'13; Bridgeland'16]*

$$(\theta_\star(\gamma), \gamma') = \langle \gamma', \gamma \rangle \quad \Leftrightarrow \quad \theta_i = -\sum_{a:i\to j} N_j$$

Let $\Omega_\star(\gamma) := \Omega_{\theta_\star(\gamma)}(\gamma)$ be the attractor invariant.

- Easy fact: for quivers without oriented loops, the only non-vanishing attractor invariants are supported on basis vectors associated to simple representations, $\Omega_\star(\gamma_i) = 1$.
- The consistency of $\mathcal{D}(Q, W)$ uniquely determines all rays in terms of the initial rays $\mathcal{R}_\star(\gamma)$, defined as those which contain $\theta_\star(\gamma)$.
- The Flow Tree Formula of *[Alexandrov BP'18]* determines the indices of outgoing rays produced by scattering initial rays *[Argüz Bousseau '20]*.

Quivers for local CY3

- Whenever a CY threefold X admits a (strong, full, cyclic) exceptional collection E, the category $D^b \operatorname{Coh} X$ is isomorphic to the category $D^b \operatorname{Rep}(Q, W)$ of representations of the quiver with potential associated to E. *[Bondal'90]*
- When X is toric, there is a simple prescription to obtain (Q, W) from brane tilings/periodic quivers. Eg. for $X = K_{\mathbb{P}^2}$,

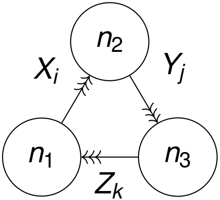

$$W = \sum \epsilon_{ijk} X_i Y_j Z_k$$

$$\gamma := [r, c_1, \mathrm{ch}_2]$$

$$\gamma_1 = [-1, 0, 0]$$
$$\gamma_2 = [2, -1, -\tfrac{1}{2}]$$
$$\gamma_3 = [-1, 1, -\tfrac{1}{2}]$$

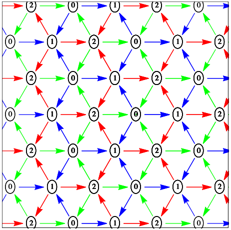

Attractor invariants for $K_{\mathbb{P}^2}$

- By studying expected dimension of the moduli space of semi-stable representations $\mathcal{M}_\theta(\gamma)$, *[Beaujard BP Manschot'20]* conjectured that the attractor index $\Omega_\star(\gamma)$ vanishes unless $\gamma = \gamma_i$ or γ lies in the kernel of the Dirac pairing, $\langle \gamma, - \rangle = 0$.
- For toric local del Pezzo surfaces, this conjecture was tested and refined by *[Mozgovoy BP '20]* and *[Descombes'21]*: $\Omega_\star(\gamma) = 0$ unless $\gamma = \gamma_i$ or $\gamma = k[D0]$, with $\Omega(k[D0]) = -y^3 - b_2 y - 1/y$. This is now a theorem for $X = K_{\mathbb{P}^2}$ *[Bousseau Descombes Le Floch BP'22]*.
- This allows to construct the quiver scattering diagram inductively, and describe any BPS state in terms of attractor flow trees.

Quiver scattering diagram for $K_{\mathbb{P}^2}$

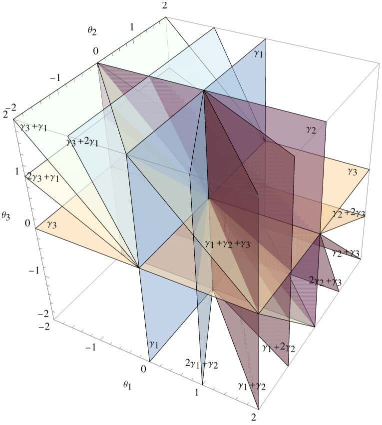

A 2D slice of the orbifold scattering diagram

Let $\mathcal{D}_o$ be the restriction of $\mathcal{D}(Q, W)$ to the hyperplane $\theta_1 + \theta_2 + \theta_3 = 1$:

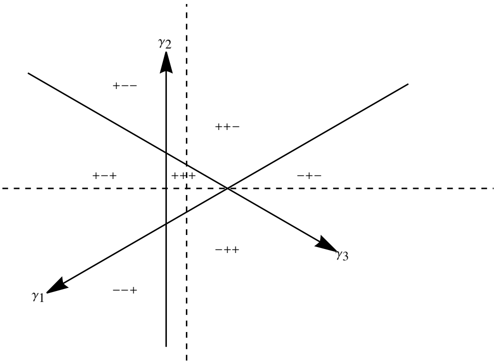

A 2D slice of the orbifold scattering diagram

Let $\mathcal{D}_o$ be the restriction of $\mathcal{D}(Q, W)$ to the hyperplane $\theta_1 + \theta_2 + \theta_3 = 1$:

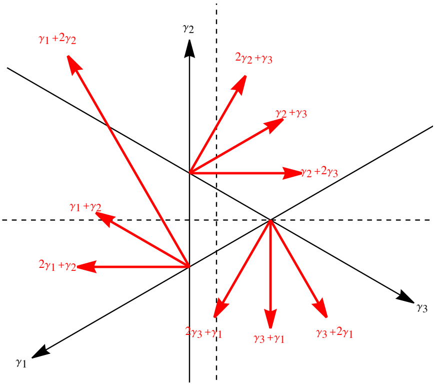

A 2D slice of the orbifold scattering diagram

Let $\mathcal{D}_o$ be the restriction of $\mathcal{D}(Q, W)$ to the hyperplane $\theta_1 + \theta_2 + \theta_3 = 1$:

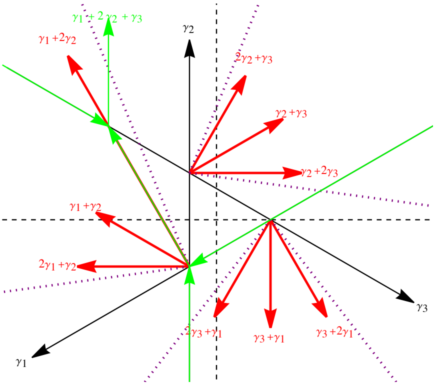

A 2D slice of the orbifold scattering diagram

The full scattering diagram $\mathcal{D}_o$ includes regions with dense set of rays:

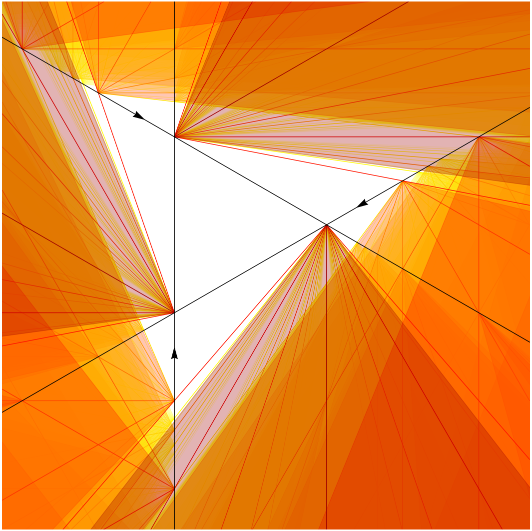

Bridgeland stability conditions

- More generally, Donaldson-Thomas invariants are defined in Bridgeland's framework of stability conditions on a triangulated CY3 category $\mathcal{C}$.
- A stability condition is a pair $\sigma = (Z, \mathcal{A})$ where $Z : \Gamma \to \mathbb{C}$ is a linear map and $\mathcal{A} \subset \mathcal{C}$ an Abelian subcategory (heart of t-structure) satisfying various axioms, e.g. $\mathrm{Im} Z(\gamma(E)) \geq 0 \; \forall E \in \mathcal{A}$.
- When it is not empty, the space $\mathrm{Stab}\,\mathcal{C}$ is a complex manifold of dimension $d = \dim K(\mathcal{C}) = \dim H^{\rm even}_{cpt}(X)$. For $X = K_S$, $d = 1 + b_2(S) + 1$.
- The group $\widetilde{GL(2,\mathbb{R})}^+$ acts on $\mathrm{Stab}\,\mathcal{C}$ by linear transformations of $(\mathrm{Re} Z, \mathrm{Im} Z)$ with positive determinant, tilting $\mathcal{A}$ accordingly, and leaves $\Omega_\sigma(\gamma)$ invariant. This effectively reduces the dimension to $d - 2 = b_2(S) = \dim \mathcal{M}_K$.

Scattering diagrams on triangulated categories

- For a general triangulated category $\mathcal{C}$, define the scattering diagram $\mathcal{D}_\psi(\mathcal{C})$ as the union of codimension-one loci in $\mathrm{Stab}\,\mathcal{C}$,

$$\mathcal{R}_\psi(\gamma) = \{\sigma : \arg Z(\gamma) = \psi + \tfrac{\pi}{2},\ \bar{\Omega}_Z(\gamma) \neq 0\}$$

  equipped with the (suitably regularized) automorphism

$$\mathcal{U}_\sigma(\gamma) = \exp\left(\frac{\bar{\Omega}_\sigma(\gamma)}{y^{-1}-y}\mathcal{X}_\gamma\right) = \mathrm{Exp}\left(\frac{\Omega_\sigma(\gamma)}{y^{-1}-y}\mathcal{X}_\gamma\right)$$

- The WCF ensures that the diagram $\mathcal{D}_\psi(\mathcal{C})$ is still locally consistent at each codimension-two intersection.
- A quiver description (Q, W) is valid whenever i) the simple objects in the exceptional collection are stable and ii) their central charges $Z(\gamma_i)$ lie in a common half-plane. In this region, $\mathcal{D}_\psi(\mathcal{C})$ must reduce to $\mathcal{D}(Q, W)$ upon setting $\theta_i = -\mathrm{Re}(e^{-i\psi} Z(\gamma_i))$.

Large volume scattering diagram

- Consider the large volume slice with quadratic central charge

$$Z^{\mathrm{LV}}(\gamma) = -rT_D + dT - \mathrm{ch}_2, \quad T_D = \frac{1}{2}T^2, \quad T = s + \mathrm{i}t$$

- Since $\mathrm{Re}Z(\gamma) = \frac{1}{2}r(t^2 - s^2) + ds - \mathrm{ch}_2$ that each ray $\mathcal{R}_0(\gamma)$ is contained in a branch of hyperbola asymptoting to $t = \pm(s - \frac{d}{r})$ for $r \neq 0$, or a vertical line when $r = 0$. Walls of marginal stability $\mathcal{W}(\gamma, \gamma')$ are half-circles centered on real axis.

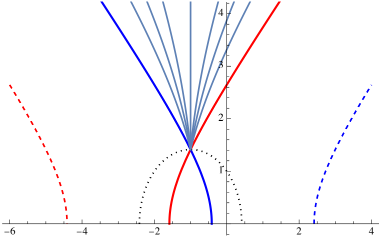

Large volume scattering diagram

- The objects $\mathcal{O}(m)$ and $\mathcal{O}(m)[1]$ are known to be stable throughout the large volume slice *[Arcara Bertram (2013)]*. The corresponding rays are 45 degree lines ending at $s = m$.
- The region of validity of the orbifold exceptional collection and its mutations covers the vicinity of the boundary at $t = 0$, hence there can be no other initial ray. *[Bousseau'19]*.

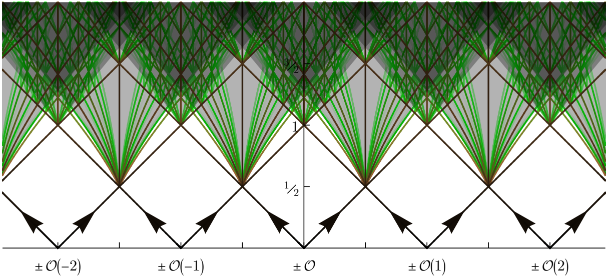

Scattering diagram in affine coordinates

Actually, Bousseau used different coordinates such that the rays become line segment $rx + dy - \mathrm{ch}_2 = 0$. This works for any ψ:

$$x := \frac{\mathrm{Re}\left(e^{-\mathrm{i}\psi} T\right)}{\cos\psi}\,, \quad y := -\frac{\mathrm{Re}\left(e^{-\mathrm{i}\psi} T_D\right)}{\cos\psi} > -\frac{1}{2}x^2$$

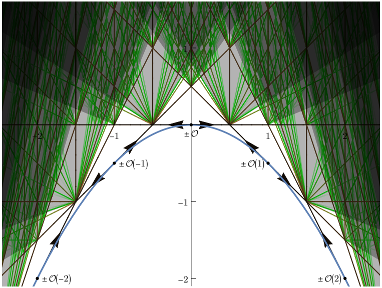

Flow tree formula at large radius

- This implies that all BPS states at large volume must arise as bound states of fluxed D4 and anti D4-branes. *How can one find the possible constituents for given* γ *and* (s,t) *?*
- Think of $\mathcal{R}(\gamma)$ as the worldline of a fictitious particle of charge r, mass $M^2 = \frac{1}{2}d^2 - r\,\mathrm{ch}_2$ moving in a constant electric field. This makes it clear that constituents must lie in the past light cone.
- Moreover, the 'electric potential' $\varphi_s(\gamma) = d - sr = \mathrm{Im} Z_\gamma / t$ increases along the flow. The first scatterings occur after a time $t \geq \frac{1}{2}$, after each constituent $k_i \mathcal{O}(m_i)$ has moved by $|\Delta s| \geq \frac{1}{2}$, by which time $\varphi_s(\gamma_i) \geq |k_i|/2$.
- Since $\varphi_s(\gamma)$ is additive at each vertex, this gives a bound on the number and charges of constituents contributing to $\Omega_{(s,t)}(\gamma)$:

$$\sum_i k_i[1, m_i, \frac{1}{2}m_i^2] = \gamma \ , \quad s - t \leq m_i \leq s + t, \quad \sum |k_i| \leq 2\varphi_s(\gamma)$$

Thus, SAFC holds along the large volume slice !

Flow trees for $\gamma = [0, 4, 1)$

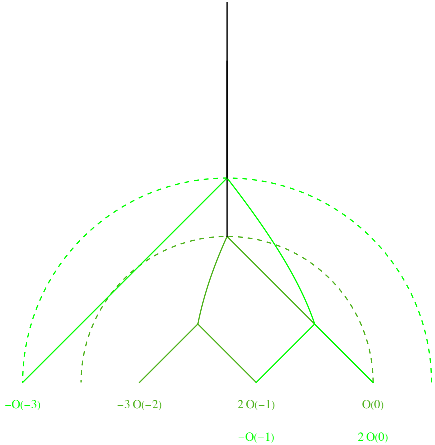

- $\{\{-3\mathcal{O}(-2), 2\mathcal{O}(-1)\}, \mathcal{O}\}$: $K_3(2,3)K_{12}(1,1) \to -156$
- $\{-\mathcal{O}(-3), \{-\mathcal{O}(-1), 2\mathcal{O}\}\}$: $K_3(1,2)K_{12}(1,1) \to -36$

Total: $\Omega_\infty(\gamma) = -192 = GV_4^{(0)}$

Flow trees for $\gamma = [1, 0, -3)$

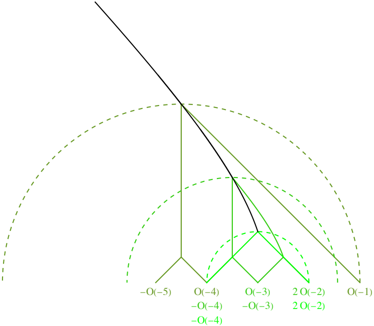

- $\{\{-\mathcal{O}(-5), \mathcal{O}(-4)\}, \mathcal{O}(-1)\}$
  $K_3(1,1)^2 \to 9$
- $\{\{-\mathcal{O}(-4), \mathcal{O}(-3)\},$
  $\{-\mathcal{O}(-3), 2\mathcal{O}(-2)\}\}$
  $K_3(1,1)^2 K_3(1,2) \to 27$
- $\{-\mathcal{O}(-4), 2\mathcal{O}(-2)\}$
  $K_6(1,2) \to 15$

Total: $\Omega_\infty(\gamma) = 51 = \chi(\mathrm{Hilb}_4 \mathbb{P}^2)$

Large volume scattering diagram for local $\mathbb{F}_0$

- For $S = \mathbb{F}_0 = \mathbb{P}^1 \times \mathbb{P}^1$, the space of Bridgeland stability conditions (modulo $GL(2,\mathbb{R})^+$) is parametrized by the Kähler moduli T_1, T_2. We focus on the canonical polarization where $\mathrm{Im}\, T_1 = \mathrm{Im}\, T_2$, and set $T_1 = T = x + \mathrm{i}t$, $T_2 = T + m$ with m real.
- The large volume slice is given by

$$Z^{\mathrm{LV}}(\gamma) = -rT(T+m) + d_1 T + d_2(T+m) - \mathrm{ch}_2$$

  The geometric rays are similar as for local $\mathbb{P}^2$, with $[r, d, \mathrm{ch}_2]$ replaced by $[2r, d_1 + d_2 - mr, \mathrm{ch}_2 - md_2]$. Set $\psi = 0$ for simplicity.
- The objects $\mathcal{O}(d_1, d_2)$, $\mathcal{O}(d_1, d_2)[1]$ are stable throughout the large volume slice *[Arcara Miles'14]*. The rays $\mathcal{R}_0(\mathcal{O}(d_1, d_2))$ start at $x = \min(d_1 - m, d_2)$ and bend to the left. Similarly, $\mathcal{R}_0(\mathcal{O}(d_1, d_2)[1]$ start at $x = \max(d_1 - m, d_2)$ and bend right.

Large volume scattering diagram for local $\mathbb{F}_0$

- The category $D^b\,\mathrm{Coh}\,X$ is isomorphic to the derived category of representations for the quiver (or one of its mutations)

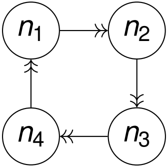

$$W = \sum_{\substack{(\alpha\beta)\in S_2 \\ (\gamma\delta)\in S_2}} \mathrm{sgn}(\alpha\beta)\,\mathrm{sgn}(\gamma\delta)\,\Phi_{12}^{\alpha}\,\Phi_{23}^{\gamma}\,\Phi_{34}^{\beta}\,\Phi_{41}^{\delta}$$

$$\begin{aligned} \gamma &:= [r, d_1, d_2, \mathrm{ch}_2] \\ \gamma_1 &= [1, 0, 0, 0] \\ \gamma_2 &= [-1, 1, 0, 0] \\ \gamma_3 &= [-1, -1, 1, 1] \\ \gamma_4 &= [1, 0, -1, 0] \end{aligned}$$

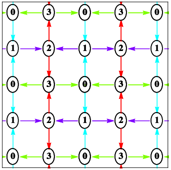

- The validity of the (mutated, shifted) quiver near $t = 0$ allows to rule out other initial rays beyond $\mathcal{O}(d_1, d_2)$ and $\mathcal{O}(d_1, d_2)[1]$.

Le Floch BP Raj, to appear

Initial rays for local $\mathbb{F}_0$ at large volume

In (x, t) coordinates, $\psi = 0$, $m = 1/2$:

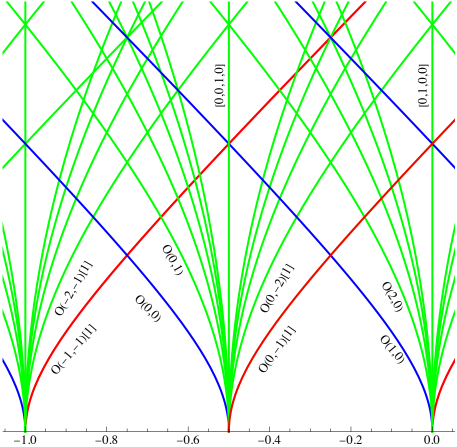

Initial rays for local $\mathbb{F}_0$ at large volume

In (x, y) coordinates, $\psi = 0$, $m = 1/2$:

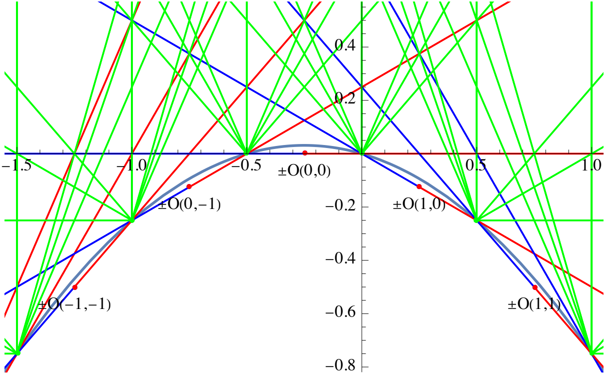

The infinite sets of rays originating from $x \in \mathbb{Z}$ and $x = \mathbb{Z} - m$ come from the scattering of two rays $\mathcal{R}(\gamma_1), \mathcal{R}(\gamma_2)$ with $\langle \gamma_1, \gamma_2 \rangle = 2$ below the parabola !

Kähler moduli space

- Mirror symmetry selects a particular Lagrangian subspace $\Pi \subset \mathsf{Stab}\,\mathcal{C}$ in the space of Bridgeland stability conditions.
- For local del Pezzo surfaces, the mirror CY3 is (a conic bundle over) a genus one curve Σ. (T_i, T_D) are given by periods of a holomorphic differential with logarithmic singularities, and satisfy Picard-Fuchs equations.
- Rather than working with flat coordinates T_i, it is advantageous to use (τ, m_i) where τ parametrizes the Coulomb branch while m_i are mass parameters in the 5D gauge theory.
- Near the large volume point, mirror symmetry ensures that $Z_\tau(\gamma) \sim \underbrace{-\int_S}\, e^{-\tau H}\, \mathrm{Td}(S)\, \mathrm{ch}(E)$, up to worldsheet instantons. Using $GL(2,\mathbb{R})^+$, one can absorb the corrections and use the simpler form $Z_\tau(\gamma) = -\int_S e^{-\tau H}\, \mathrm{ch}(E)$.

Modularity in Kähler moduli space

- In some cases, the monodromy group is a subgroup $\Gamma \subset SL(2,\mathbb{Z})$, and the universal cover of $\mathcal{M}_K = \mathbb{H}/\Gamma$ becomes the Poincaré half-plane $\mathbb{H}$. *[Closset Magureanu'21; Aspman Furrer Manschot'21]*
- This happens for $X = K_{\mathbb{P}^2}$, where $\Gamma = \Gamma_1(3)$, and for $X = K_{\mathbb{F}_0}$ at special points $m \in \mathbb{Z}$ where $\Gamma = \Gamma_0(8)$. For generic m, $\Gamma = \Gamma_1(4)$ with a square root branch cut.

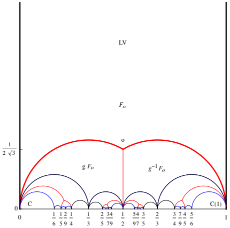

$K_{\mathbb{P}^2} : \Gamma_1(3)$

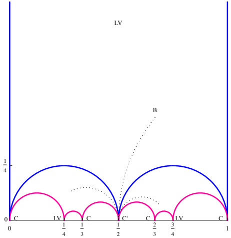

$K_{\mathbb{F}_0} : \Gamma_1(4)$

Central charge as Eichler integral

- One can show that $(\partial_\tau T, \partial_\tau T_D)$ are proportional to the periods $(1,\tau)$ of the mirror curve. Integrating along a path from reference point o to τ, one finds an Eichler integral representation

$$\begin{pmatrix} T \\ T_D \end{pmatrix} = \begin{pmatrix} T^o \\ T_d^o \end{pmatrix} + \int_{\tau_o}^{\tau} \begin{pmatrix} 1 \\ u \end{pmatrix} C(u)\,\mathrm{d}u$$

where $C(\tau)$ is a weight 3 modular form:

$$C_{\mathbb{P}^2} = \frac{\eta(\tau)^9}{\eta(3\tau)^3}, \quad C_{\mathbb{F}_0} = \frac{\eta(\tau)^4\eta(2\tau)^6}{\eta(4\tau)^4}\sqrt{\frac{J_4+8}{J_4+8\cos\pi m}}$$

Here $J_4(\tau) = 8 + \left(\frac{\eta(\tau)}{\eta(4\tau)}\right)^8$ is the Hauptmodul for $\Gamma_1(4)$.

Central charge as Eichler integral

- This provides an computationally efficient analytic continuation of Z_τ throughout $\mathbb{H}$, and gives access to monodromies:

$$\tau \mapsto \frac{a\tau+b}{c\tau+d} \quad \begin{pmatrix} 1 \\ T \\ T_D \end{pmatrix} \mapsto \begin{pmatrix} 1 & 0 & 0 \\ f & d & c \\ e & b & a \end{pmatrix} \cdot \begin{pmatrix} 1 \\ T \\ T_D \end{pmatrix}$$

  where (e,f) are period integrals of C from τ_o to $\frac{d\tau_o-b}{a-c\tau_o}$.
- At large volume $\tau \to \mathrm{i}\infty$, using $C = 1 + \mathcal{O}(q)$ one finds

$$T = \tau + \mathcal{O}(q), \quad T_D = \frac{1}{2}\tau^2 + \frac{1}{8} + \mathcal{O}(q)$$

  in agreement with $Z_\tau(\gamma) \sim -\int_S e^{-\tau H}\,\mathrm{Td}(S)\,\mathrm{ch}(E)$.

Exact scattering diagram for $K_{\mathbb{P}^2}$

- The scattering diagram $\mathcal{D}^{\Pi}_{\psi}$ along the physical slice should interpolate between $\mathcal{D}^{\rm LV}_{\psi}$ around $\tau = i\infty$ and $\mathcal{D}_o$ around $\tau = \tau_o$, and be invariant under the action of $\Gamma_1(3)$.
- Under $\tau \mapsto \frac{\tau}{3n\tau+1}$ with $n \in \mathbb{Z}$, $\mathcal{O} \mapsto \mathcal{O}[n]$. Hence there is a doubly infinite family of initial rays emitted at $\tau = 0$, associated to $\mathcal{O}[n]$.

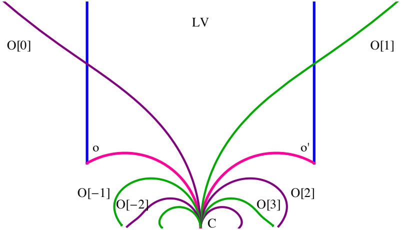

- Similarly, there must be an infinite family of initial rays coming from $\tau = \frac{p}{q}$ with $q \neq 0 \mod 3$, corresponding to $\Gamma_1(3)$-images of $\mathcal{O}$, where an object denoted by $\mathcal{O}_{p/q}$ becomes massless.

Exact scattering diagram for small ψ

- For $|\psi|$ small enough, the only rays which reach the large volume region are those associated to $\mathcal{O}(m)$ and $\mathcal{O}(m)[1]$. Thus, the scattering diagram $\mathcal{D}^{\Pi}_{\psi}$ is isomorphic to $\mathcal{D}^{\rm LV}_0$ inside $\mathcal{F}$ and its translates:

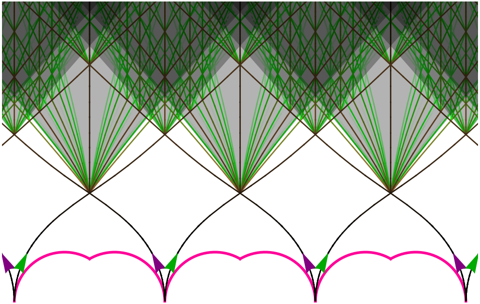

Scattering diagram in affine coordinates

- In affine coordinates, the initial rays $\mathcal{R}_{\mathcal{O}(m)}$ are still tangent to the parabola $y = -\frac{1}{2}x^2$ at $x = m$, but the origin of each ray is shifted to $x = m + \mathcal{V}\tan\psi$ where $\mathcal{V}$ is the quantum volume

$$\mathcal{V} = \mathrm{Im}\, T(0) = \frac{27}{4\pi^2}\mathrm{Im}\left[\mathrm{Li}_2(e^{2\pi\mathrm{i}/3})\right] \simeq 0.463$$

- The topology of $\mathcal{D}^{\Pi}_{\psi}$ jumps at a discrete set of rational values

$$\mathcal{V}\tan\psi \in \{\tfrac{F_{2k}+F_{2k+2}}{2F_{2k+1}}, k \geq 0\} = \{\tfrac{1}{2}, 1, \tfrac{11}{10}, \tfrac{29}{26}, \tfrac{19}{17}, \dots\}$$

and a dense set of values in $[\frac{\sqrt{5}}{2}, +\infty)$ where secondary rays pass through a conifold point.

Affine scattering diagram, $|\mathcal{V} \tan\psi| < 1/2$

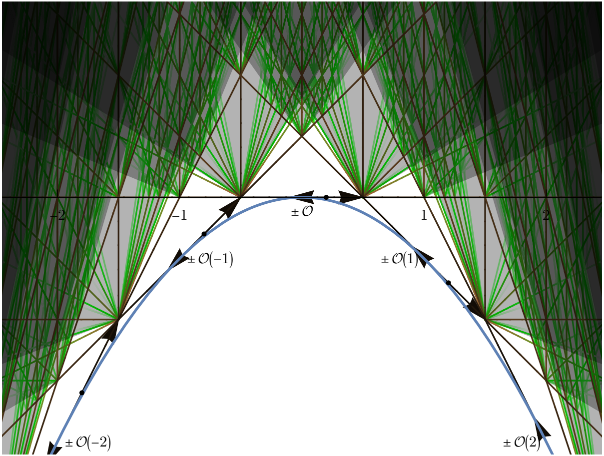

Exact scattering diagram, $\psi = 0$

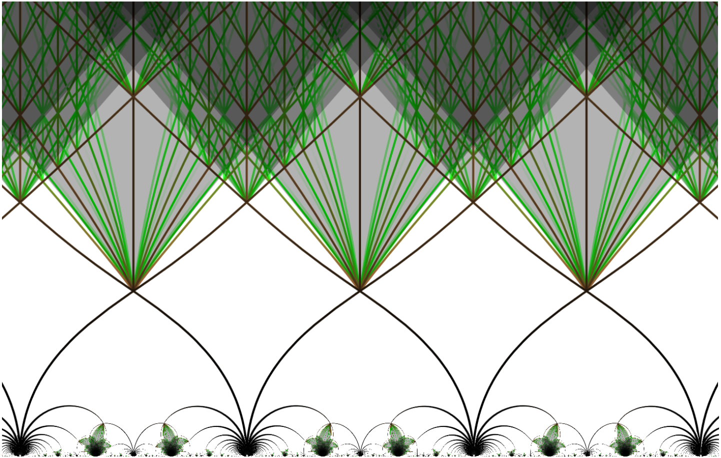

Exact scattering diagram, $\psi = 0.3$

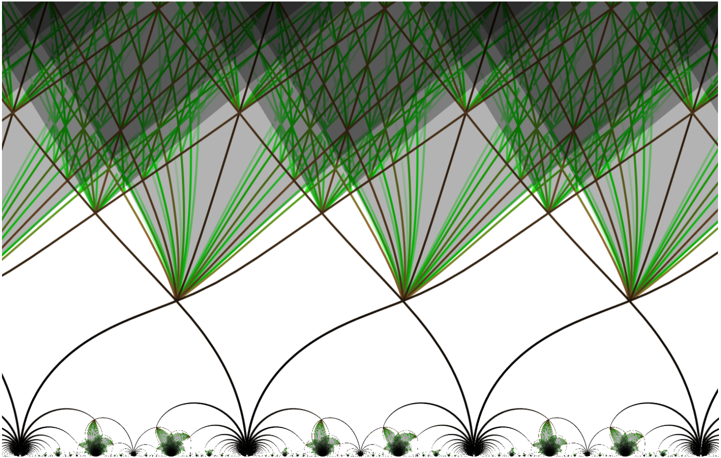

Exact scattering diagram, $\psi = 0.6$

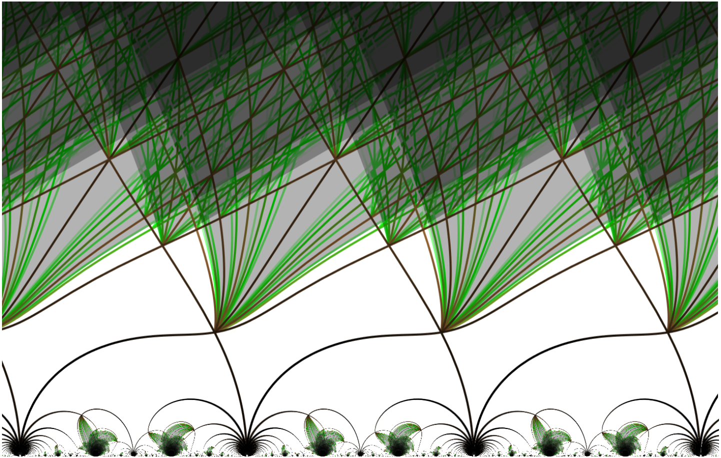

Exact scattering diagram, $\psi = 0.8$

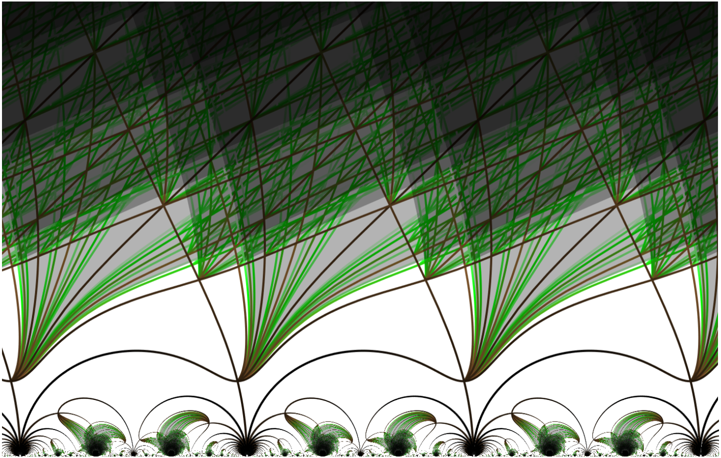

Exact scattering diagram, $\psi = 0.824$

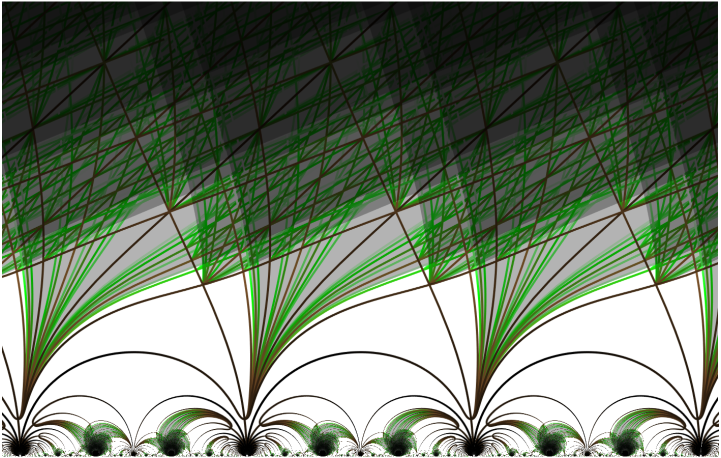

Exact scattering diagram, $\psi = 0.825$

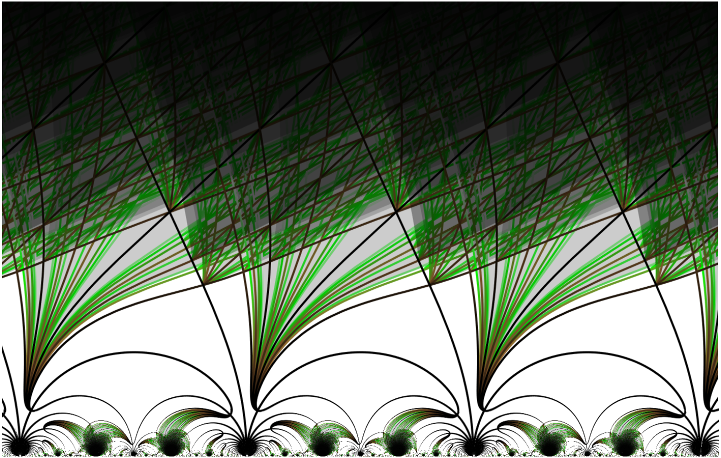

Exact scattering diagram, $\psi = 0.9$

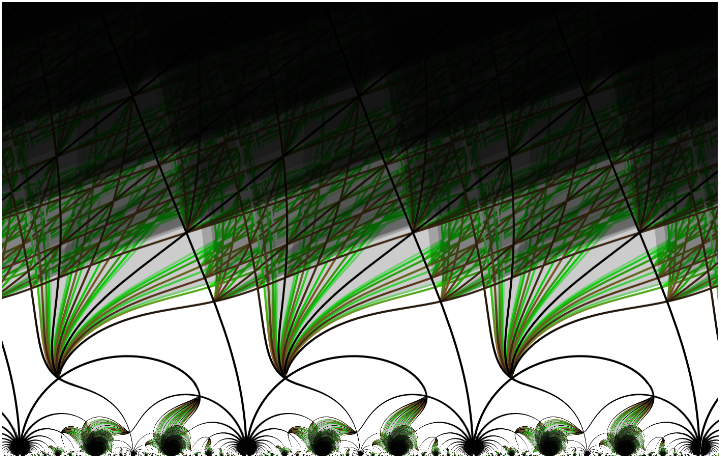

Exact scattering diagram, $\psi = 1$

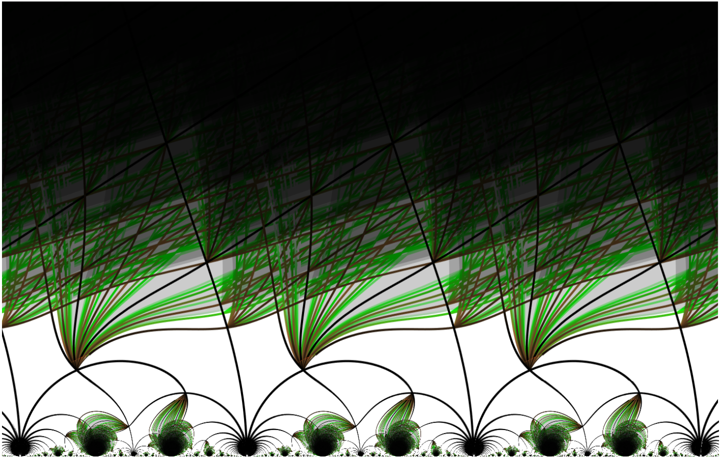

Exact scattering diagram, $\psi = 1.137$

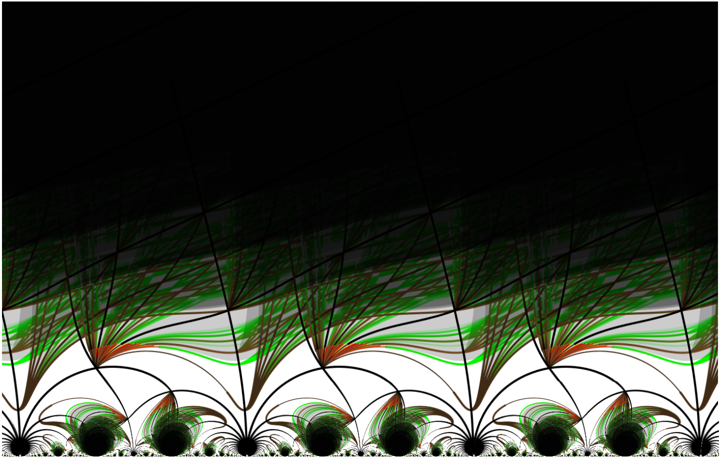

Exact scattering diagram, $\psi = 1.139$

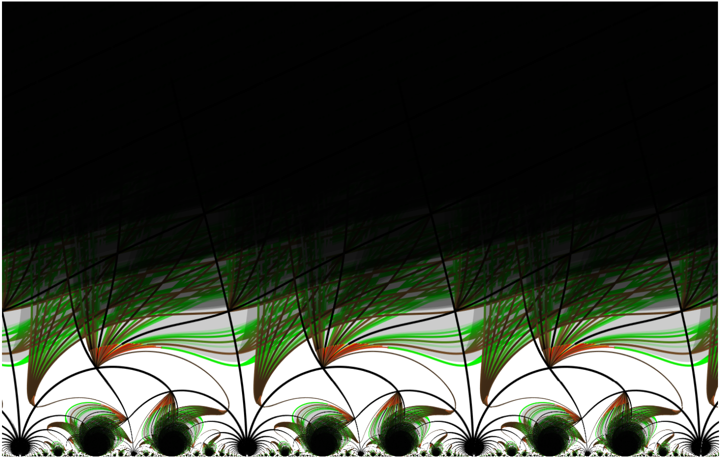

Exact scattering diagram, $\psi = \pi/2$

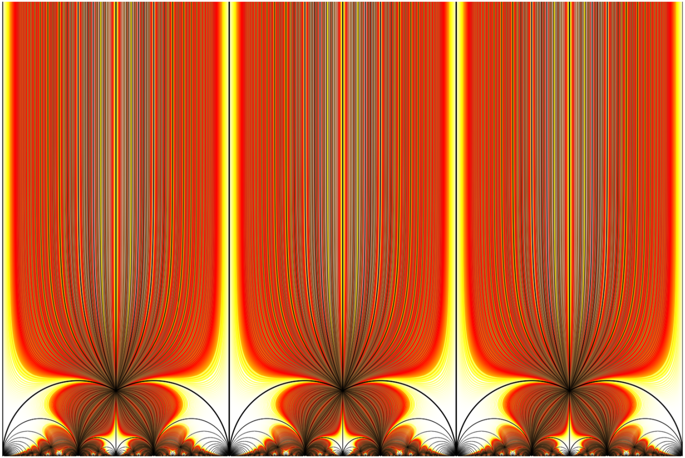

Exact scattering diagram for $\psi = \pm\frac{\pi}{2}$

- For $\psi = \pm\frac{\pi}{2}$, the geometric rays $\{\mathrm{Im} Z_\tau(\gamma) = 0\}$ coincide with lines of constant $s := \frac{\mathrm{Im}\, T_D}{\mathrm{Im}\, T} = \frac{d}{r}$, independent of ch_2:

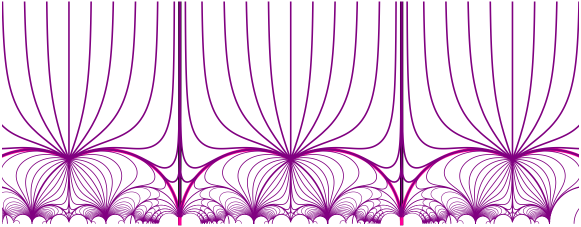

- Hence, there is no wall-crossing between τ_o and $\tau = \mathrm{i}\infty$ when $-1 \leq \frac{d}{r} \leq 0$, explaining why the Gieseker index $\Omega_\infty(\gamma)$ agrees with the quiver index $\Omega_c(\gamma)$ in the anti-attractor chamber.

Douglas Fiol Romelsberger'00, Beaujard BP Manschot'20

Fake walls and bound state metamorphosis

$\gamma = [0, 1, 1) = \mathrm{ch}\, \mathcal{O}_C$: $\Omega_{t\gg 1} = K_3(1,2) K_3(1,3)^{n-1} = y^2 + 1 + 1/y^2$

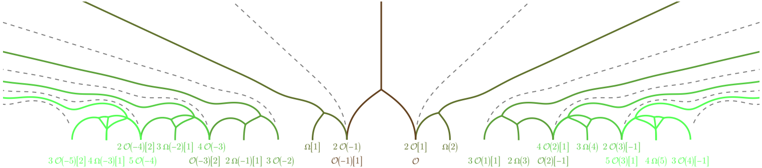

$\gamma = [1, 0, 1) = \mathrm{ch}\, \mathcal{O}$: $\Omega_{t\gg 1} = K_3(1,3) \dots K_3(1,3n) = 1$

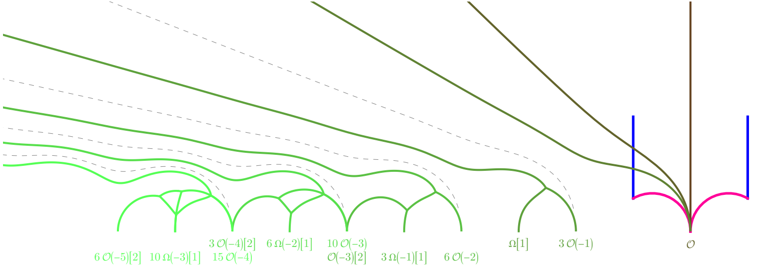

Exact scattering diagram for $K_{\mathbb{F}_0}$

- For local $\mathbb{F}_0$, the scattering diagram is complicated by branch cuts and m-dependence. The quantum volume is now

$$T(0) = \mathrm{i}\mathcal{V}(m) = \frac{2}{\pi^2}\left(\mathrm{Li}_2(\mathrm{i}e^{\mathrm{i}\pi m/2}) - \mathrm{Li}_2(-\mathrm{i}e^{\mathrm{i}\pi m/2})\right)$$

In (x, y) coordinates, the origin of the initial rays is shifted by $\Delta x = \tan\psi\,\mathrm{Re}\mathcal{V}(m) - \mathrm{Im}\mathcal{V}(m)$.

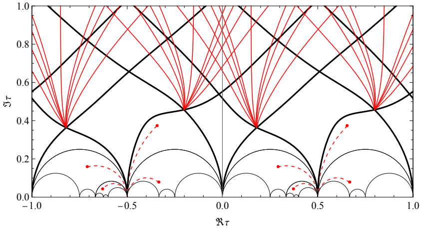

Large volume scattering diagram for $K_{\mathbb{F}_1}$

- Viewing $\mathbb{F}_1$ as a one-point blow-up of $\mathbb{P}^2$, $H^2(S,\mathbb{Z}) = H\mathbb{Z} + C\mathbb{Z}$ with $H^2 = 1, C^2 = -1, H.C = 0$, $K_S = C - 3H$.
- The exceptional collection $(\mathcal{O}, \mathcal{O}(H-C), \mathcal{O}(H), \mathcal{O}(2H-C))$ leads to a quiver description:

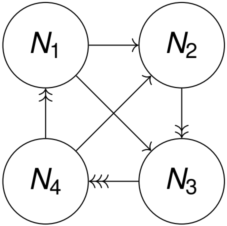

$$
\begin{aligned}
\gamma_1 &= [1,0,0,0] \\
\gamma_2 &= [-1,1,-1,0] \\
\gamma_3 &= [-1,0,1,1/2] \\
\gamma_4 &= [1,-1,0,1/2]
\end{aligned}
$$

- Due to the existence of a curve C with negative self-intersection, the fluxed D4-branes are no longer absolutely stable !

Large volume scattering diagram for $K_{\mathbb{F}_1}$

- Indeed, rays inside the shaded quiver regions below are ruled out:

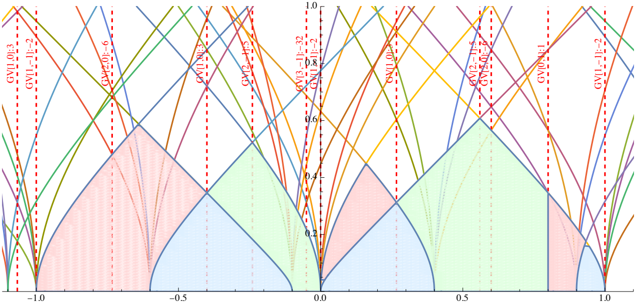

Large volume scattering diagram for $K_{\mathbb{F}_1}$

- Initial rays for $0 < m < \frac{1}{4}$ are

$$\mathcal{O}, \mathcal{O}(H-C), \mathcal{O}(H), \mathcal{O}(2H-C)$$

tensored with arbitrary powers of $K_S = \mathcal{O}(C-3H)$. Remarkably, these form the foundation of an helix ! *[Bondal, Rudakov'90]*

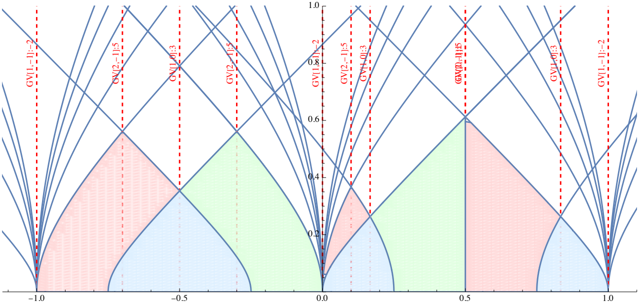

Scattering diagram for $K_{\mathbb{F}_1}$ in affine coordinates

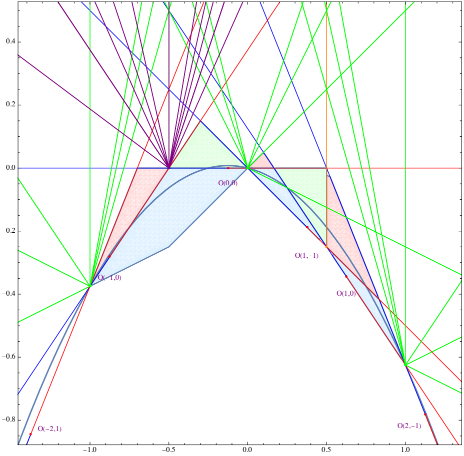

Conclusion - outlook

- Scattering diagrams provide an efficient way to organize the BPS spectrum, on local CY3 manifolds, and a natural decomposition into elementary constituents.
- It would be interesting to extend this description to other toric CY3, such as higher del Pezzo surfaces. We expect that initial rays in the large volume slice will be controlled by helices.
- Unfortunately, 5D SCFTs with modular Coulomb branches are rare ! *[Closset Magureanu'21-22]*
- For compact CY3, $Z(\gamma) = e^{K/2} Z_{\rm hol}(\gamma)$ is not longer holomorphic, so $\arg Z(\gamma)$ is not constant along the flow, and there can be rays originating from regular attractor points. Can one nonetheless use scattering diagrams to organize the BPS spectrum ?

Thanks for your attention !